Lawrence Berkeley National Laboratory
LBL Publications

Title

Development, implementation and performance of a model predictive controller for packaged air conditioners in small and medium-sized commercial building applications

Permalink

https://escholarship.org/uc/item/0kk608vf

Authors

Kim, Donghun
Braun, James E

Publication Date

2018-11-01

DOI

10.1016/j.enbuild.2018.08.019

Peer reviewed

eScholarship.org Powered by the California Digital Library
University of California

Development, Implementation and Performance of a Model Predictive Controller for Packaged Air Conditioners in Small and Medium-sized Commercial Building Applications

Donghun Kim[a,*], James E. Braun[a]

[a]*School of Mechanical Engineering, Purdue University, West Lafayette, IN, USA*

Abstract

Small and medium sized commercial buildings, such as retail stores, restaurants and factories, often utilize multiple packaged air conditioners, i.e. roof top units (RTUs), to provide cooling and heating for open spaces. A conventional control approach for these buildings relies on local feedback control, where each unit is cycled on and off using its own thermostat. The lack of coordination between RTUs represents a missed opportunity for operating more efficient units when there is strong coupling between the spaces they serve and can lead to unnecessarily high electrical demand due to the inherent randomness of unit cycling. This paper presents an overall model-based predictive control (MPC) approach for RTU coordination that includes a description of the control architecture, modeling approach, implementation, and assessment. We provide results of laboratory and field tests that demonstrate the short-term and long-term performance of the MPC solution in terms of energy and demand savings.

Keywords: Model predictive control, MPC, building control, RTU control, packaged air conditioner

1. Introduction

Over one third of the total number of small ($< 464m^2$, $< 5,000ft^2$), and medium-sized ($< 4,640m^2$, $< 50,000ft^2$) commercial buildings across the U.S., such as banks, retail stores, restaurants and factories, are served by multiple packaged rooftop units (RTU) for space heating and cooling (DOE, 2009). Most of these units are controlled independently using a simple thermostat control where each RTU is cycled on and off based on its own thermostat. This localized control can lead to poor coordination among the RTUs and it is very likely that all of the units within a building would sometimes be operating simultaneously,

*Corresponding author
Email address: kim1077@purdue.edu (Donghun Kim)

even for part load conditions, resulting in high electric peak demand and short cycling. Furthermore, there is often a strong coupling between the spaces served by RTUs in these types of buildings creating opportunities for preferentially operating the most efficient units with minimal impact on comfort.

Small and medium-sized commercial buildings (SMCB) have not been a major focus for building control researchers and developers in the past, mainly because they tend not to have building automation systems (BAS) and because the cost savings opportunities relative to implementation costs have been small. According to Katipamula et al. (2012), over 90% of small and medium-sized commercial buildings currently do not have a BAS. However, the situation is changing because of the availability of low-cost, web-enabled smart thermostats and other devices (e.g., smart plugs) that have emerged in the marketplace in the past few years. Even with this low-cost energy management platform, there is a need for control approaches that have low implementation requirements and costs.

Recently, there have been some developments and applications of advanced supervisory controller for multiple rooftop packaged units (RTUs) with demonstrations of significant energy and demand savings opportunities. **?** developed a MPC algorithm and implemented it at a gymnasium having four identical 10-ton RTUs. This coordinator combines a simplified ARX type input-output model with heuristics and optimization to limit electric peak demand. The reduction of peak power consumption was about 15% with respect to a conventional thermostat control for the building. Kim et al. (2015) developed a MPC algorithm for minimizing energy consumption and electric peak demand for multiple RTUs especially for open-spaced buildings. The control approach was designed to minimize sensor and configuration requirements in order to enable a more cost effective control implementation for the small/medium commercial building. About 20% building HVAC energy savings and about 30% peak demand reduction were reported for a small commercial building. Biyik et al. (2015) developed a RTU coordinator to minimize peak power. The goal was achieved by assigning different time varying penalties to different RTUs in order to prevent all units from operating simultaneously. It is reported that the peak power reduction with the optimal control strategy was about 20-40% for existing buildings. Putta et al. (2015) applied dynamic programming to solve an optimization problem for minimizing energy consumption and reducing compressor short cycling. In the case study, about 10% energy savings were estimated for a building served by 4 RTUs. Zhang et al. (2017) developed a RTU coordination control algorithm that shaves power usage within a limit during a demand response event for 90 minutes when triggered by a electric utility, while minimizing comfort impacts.

Despite these developments, there is a need tor complete and fully validated MPC solutions for SMCBs that can be implemented at low cost and are robust and reliable. So far, the savings were estimated either using simulations or using short period experiments, from a couple of hours to a couple of weeks. However, to have increased reliability for successful market penetration, more demonstrations over a long period at field sites are necessary.

This paper presents and demonstrates an MPC solution for coordinating RTUs in SMCBs that is an extension of the work previously presented by Kim et al. (2015). There are a number of new contributions. First of all, the cost function and constraints are modified to accommodate optimal control coordination when RTUs serve separate spaces that don't have close thermal coupling (e.g., office buildings). These types of buildings have significant opportunities for demand reduction with some energy savings through optimal coordination of the cycling patterns. The previous work focused on open spaces served by multiple RTUs. Second of all, this paper presents a complete control solution that includes a model identification approach, a MPC algorithm and control architecture. The previous work focused on the MPC algorithm. Third of all, the current work provides a much more complete demonstration and evaluation of the control approach that includes both laboratory test results and long-term performance assessments of the MPC implementation at a field site. In Section 2, characteristics of small and medium-sized commercial buildings and some challenges for applying MPC to those buildings are outlined. The overall MPC design approach is presented in Section 3 that is focused on handling unmeasured building heat gains in modeling and control phases for a reliable MPC implementation. Section 4 shows the performance of the MPC through experiments performed in both a laboratory setting and field site.

2. System Description and MPC Challanges

An RTU is a packaged air conditioning unit consisting of a vapor compression cycle, supply air blower, air mixing box and optional economizer and heating element, i.e. an electric heater or gas burner. In general, a thermostat is dedicated to an RTU and turns one or more compressor stages on and off to maintain a local zone air temperature near a setpoint. The first stage is typically energized when the thermostat temperature falls below the setpoint by a deadband. If the temperature continues to decrease and falls below the setpoint by a 2nd stage deadband, then the 2nd stage compressor is energized. The supply fan is typically on continuously during the occupied period or can cycle with the compressor during unoccupied times. Most RTUs in the field do not have variable speed compressors or fans controlled by variable frequency drives.

To formulate the control problem for supervising the stages of multiple RTUs, let $n \in \mathbb{N}$ be the number of thermostats or equivalently the number of RTUs. The measured outputs (or controlled variables) are the thermostat temperatures, denoted as $y \in \mathbb{R}^n$. The control inputs (or manipulated variables) are RTU compressor stages, denoted as $u \in \mathbb{Z}^n$, and we assume the information of the outdoor air temperature, $T_o \in \mathbb{R}$, is available. Let $[u^T, T_o]^T$ be the measured inputs having the size of m where $m = n + 1$. The dynamics of the system, namely $G_u : u \mapsto y, G_{T_o} : T_o \mapsto y$, in nature is very complex, because it involves a refrigerant cycle, the heat exchange between ventilation air and the refrigerant, inter-zonal air flows that could vary depending on the combina-

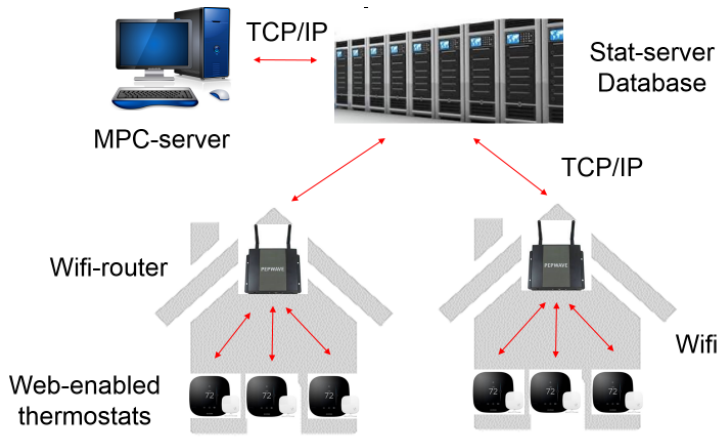

Figure 1: A conceptual schematic of a control architecture for implementing MPC for small/medium sized buildings

tion of the supply fan modes and air duct systems, and the time constants of thermostats.

The control objective is to maintain y within a temperature bound while minimizing energy consumption and electric peak demand associated with u. A significant challenge arises in applying an optimal control approach to small and medium-sized commercial buildings because of the lack of a BAS. This implies the need for a low-cost control architecture that can be retrofit in existing small/medium building applications. The overall solution should include a set of hardware and software to monitor space temperatures and control RTU operations that allows implementation of an advanced control algorithm with minimal sensor and configuration requirements.

For SMCB applications, only limited sensor information is available, e.g. y, u and T_o. This means heat gains that drive building dynamics (e.g., occupancy gains, lights, plug loads, in/exfiltration) represent significant unmeasured disturbances in a model-based control solution. It is well known that unmeasured disturbances create challenges for both modeling and control. Solving this issue is critically important in enabling a reliable MPC solution for real applications.

3. Construction of MPC for Coordinating RTUs

3.1. Proposed Control Architecture for Small/Medium Building Applications

A compact version of a BAS for small commercial building applications that was implemented in this work is shown in Fig. 1. At the bottom of the figure, web-enabled thermostats and a wifi-router are installed in each building. The web-enabled thermostats monitor and send building system operation data that include thermostat temperatures (y), ON/OFF stage or run times of RTU compressors (u), and user setpoints and schedules to a thermostat server via the

internet. The server records the measurements from all buildings in a database. The outdoor air temperature for each building is obtained from a weather station. The centralized MPC-server located at the upper left corner in the figure receives the status of all buildings in real time by communicating to the stat server, and calculates optimal decisions for each building. These decisions feed back to each thermostat via the internet.

Since the configuration of each building in the proposed control infrastructure is modular, the structure is able to accommodate a number of buildings in a scalable manner. In addition, it allows ease of management and updating an advanced control algorithm and reduces capital costs for control implementation because each building does not need to purchase a computer. All case study results presented in this paper are based on this control infrastructure with commercially available web-enabled thermostats.

3.2. Modeling: System Identification

3.2.1. Identification Problem and Challenge

In the proposed cost control architecture, u, T_o, and y are available measurements for modeling. It is assumed that measurements are collected under closed-loop operation. In other words, u is determined by a thermostat control loop. The limited sensor information implies that there are unknown but possibly significant heat gains (e.g., solar radiation and internal gains) that influence the IO data and model identification. Therefore, the modeling objective becomes to estimate G_u and G_{T_o} without information of unmeasured disturbances. In addition, the closed-loop operation implies control inputs u are correlated to the disturbances since thermostat feedback controllers have to reject the unknown heat gains. The existence of unknown inputs and the strong correlation to control inputs in an estimation dataset cause a significant challenge in modeling, and can result in a poor model (Forssell and Ljung, 1999; Van den Hof, 1998; Ljung and McKelvey, 1996; Van Overschee and De Moor, 1997). Intuitively speaking, this is because an estimated model from the dataset should explain the input and output relationships without knowledge of unmeasured heat gains.

3.2.2. Identification Approach to Alleviate Effect of Unmeasured Heat Gains

A methodology termed the lumped output disturbance modeling approach has been developed to resolve the modeling issue associated with unmeasured heat gains in building thermal systems (Kim et al., 2016, 2018). The identification approach aims at extracting an improved RC network building model from data under the presence of unknown heat gains. The approach is adopted for developing models for MPC in this work, and its key concept is outlined in this section.

A discretized thermal network model for our applications can be expressed as the following general form.

$$y(k) = G_u(z)u(k) + G_{T_o}(z)T_o(k) + G_g(z)\dot{Q}_g(k) \quad (1)$$

$\dot{Q}_g(k)$ represents the unmeasured input disturbances [kW], e.g. occupancy gains, lighting loads and transmitted solar radiation, and G_g is the corresponding transfer function that maps $\dot{Q}_g$ to y, which depends on building dynamics. From (1), one can see the difficulty to accurately extract G_u and G_{T_o} from u, T_o, y without $\dot{Q}_g$.

In the lumped output disturbance modeling approach, only the signal of $v(k)$, namely lumped output disturbances defined as $v(k) := G_g(z)\dot{Q}_g(k)$[1], is of interest, and it tends to model the process v as a stochastic process. A key observation is that v is a low pass filtered signal through the slow building dynamics of G_g, although input disturbances could have a variety of frequency contents. This suggests that v could be modeled as

$$v(k) = H(z)e(k) \tag{2}$$

with a low pass filter H. $e(\cdot)$ is a white noise process in the equation.

Therefore, the building system we wish to identify has the following form.

$$y(k) = G_u(z)u(k) + G_{T_o}(z)T_o(k) + H(z)e(k) \tag{3}$$

A state space model structure for (3) is

$$\begin{aligned} \hat{T}(k+1) &= A(\theta)\hat{T}(k) + B_u(\theta)u(k) + B_{T,o}(\theta)T_o(k) \\ y(k) &= C(\theta)\hat{T}(k) + \hat{v}(k) \\ \hat{\zeta}(k+1) &= \mathcal{F}(\rho)\hat{\zeta}(k) + \mathcal{G}(\rho)\epsilon(k) \\ \hat{v}(k) &= \hat{\zeta}(k) + \epsilon(k) \end{aligned} \tag{4}$$

θ and ρ represent parameters for a semi-physical model that consists of thermal resistances and capacitances, and parameters for the low pass filter to characterize v, respectively. $A(\theta), B_u(\theta)$ and $B_{T_o}(\theta)$ are defined by a RC network model and discretization scheme, e.g. the zero-order hold. $\hat{T}$ contains estimated states (temperatures of zones and walls in a RC network), $\hat{v}$ is an estimation of true output disturbances, and $\hat{\zeta}$ is the internal state appearing in converting the transfer function description of the output disturbances (3) to the state space description (4). For a precise definition for each term, see Kim et al. (2018).

To retrieve θ and ρ from measurements of u, T_o, y, the prediction error method is used based on the state space form that minimizes a norm of the innovation process of ϵ in (4). In this paper, the nonlinear least square problem was solved with matlab lsqcurvefit which uses the *Levenberg-Marquardt* algorithm. To handle the non-convexity of the optimization problem, the optimization algorithm was repeated at multiple starting points.

The uniqueness of this approach compared with other grey-box modeling approaches in the building science (Andersen et al., 2000; Braun et al., 2001;

[1] Note from (1) that output disturbance v has the unit of $[^oC]$ while the input disturbance $\dot{Q}_g$ has that of $[kW]$.

Chen et al., 2015; Dong et al., 2011; Fraisse et al., 2002; Harb et al., 2016; Reynders et al., 2014; Rogers et al., 2014; Širokỳ et al., 2011) is that building disturbances are not treated as white noise, and are modeled with a grey-box model structure rather than a black box structure. Compared with disturbance modeling approaches on black-box model structures, the additional state $\hat{\zeta}$ is augmented to the physical state $\hat{T}$, and the dynamics associated with them are completely decoupled. This provides flexibility in our disturbance model $H(\rho)$ for fitting H with a smaller number of parameters. For example, ARX, ARMAX or model structures of subspace identification methods (Ljung, 1999; Söderström and Stoica, 1988) have constraints such that dynamics of a system and disturbance have shared poles while our disturbance model structure does not need to. In this sense, the proposed model structure (4) is a grey-box version of the Box-Jenkins model structure.

The identification approach has been validated for a single zone building and multi-zone building using both simulations and experiments, and resulted in significantly better models compared with a conventional grey-box identification approach. For the results, refer to Kim et al. (2016, 2018).

In this paper, it is assumed that only T_o is a measured disturbance. If other measurements, e.g. solar irradiation, are available, the treatment of unmeasured disturbances are the same, i.e. to model unmeasured disturbances as (2) and to estimate both θ and ρ. However, the RC model structure should be modified to include the additional disturbance inputs. An example of the lumped output disturbance modeling approach when both T_o and solar irradiation are available can be found in Kim et al. (2016). A technical challenge of having additional disturbance inputs is in the selection of an estimation dataset. To correctly capture input and output relationships across the various inputs, it is necessary to have data where cross correlations between inputs are small. As the number of measured disturbances increases, the decorrelation requirement becomes more challenging because disturbances are not controllable. See (Kim et al., 2018) for more detailed discussions.

3.3. Control Approach

Since a conventional thermostat control approach does not consider overall building performance, it is natural to design a controller targeting reduction of energy consumption and peak demand in a centralized manner. Previously, authors developed and demonstrated a MPC algorithm coordinating multiple RTUs (Kim et al., 2015) that has minimal sensor requirements, but the control approach is limited to buildings where several RTUs serve a big open space area, like a gymnasium. However, certain types of small and medium-sized buildings have predominantly separate zones served by different units, e.g. office buildings. In this section, we present a generalized and extended version of the MPC that can handle general types of SMCBs. The algorithm details are explained in this section.

3.3.1. Problem Formulation

The control optimization involves determining a trajectory of all RTU stages for a relatively short prediction horizon (e.g., 30 minutes) that minimizes a cost function that includes terms for energy use, peak demand, and deviation from comfort bounds. The control objective at a current time step k is:

$$\min_{u(k+j)\in\mathbb{Z}^n,\delta\in\mathbb{R}^+,\Gamma_l\in\mathbb{R}^+,\Gamma_u\in\mathbb{R}^+} \Big(\sum_{j=1}^{N_p}\sum_{i=1}^{n} p_i u_i(k+j)\Big) + d\cdot\delta + c_l\cdot\Gamma_l + c_u\cdot\Gamma_u \quad (5)$$

$$\begin{aligned} s.t. \quad & T_l - \Gamma_l \le E(y(k+N_p)|\mathcal{G}_k) \le T_u + \Gamma_u \\ & \sum_{i=1}^{n} p_i u_i(k+j) \le \delta \quad (\forall j \in \{0,\cdots,N_p-1\}) \end{aligned} \quad (6)$$

where p_i is the rated power for i^{th} unit[2], and hence the first term in the control objective represents a energy consumption over a predicted horizon, N_p. $E(y(k+N_p)|\mathcal{G}_k)$ is the optimal N_p-step prediction for y given available measurements and candidate future control inputs of $\mathcal{G}_k = \{y(k-1), y(k-2), \cdots, u(k+N_p-1), u(k+N_p-2), \cdots, u(k-1), u(k-2), \cdots\}$. T_u, T_l $(\in \mathbb{R}^n)$ are temperature upper and lower bounds, respectively. c_l, c_u $(\in \mathbb{R}^+)$ and d $(\in \mathbb{R}^+)$ are weights on optimization variables of Γ_l, Γ_u $(\in \mathbb{R}^+)$ and $\delta(\in \mathbb{R}^+)$.

For any given prediction horizon, the optimal controller tries to determine the RTU stages that would minimize power consumption. The staging is assumed to be fixed over the prediction horizon (no cycling) and thus it is appropriate to use an estimate of the steady-state power consumption for the current conditions, However, in order to eliminate the need for collecting individual RTU power consumption data (from measurements or manufacturers' performance maps) for identifying a model, rated powers for the individual RTU stages are used in the optimization. Rated power is readily available from the RTU nameplate and technical specification manual, thus requiring minimal effort for configuration. The use of rated power in the optimization would be exact if RTU power didn't depend on outdoor and indoor temperatures. However, it works works well because the different units have nearly identical indoor and outdoor conditions and the effects of variations in these boundary conditions from rating conditions on power have very similar trends for different RTUs. For more detailed discussion on the assumption of using rated power in place of measured power, refer to Kim et al. (2015).

From the last constraints of (6), it can be seen that δ is an upper bound on each instantaneous electric demand over the prediction horizon. Therefore

[2]For a multistage unit, it is assumed that the rated power for each unit behaves linearly mainly for simplicity of the problem formulation. When the stage powers are significantly different, the control formulation should be modified by replacing n with the number of stages and by defining p_i as the rated power for i^{th} stage not i^{th} unit. Refer to Kim et al. (2015) for a clearer formulation.

minimizing δ will naturally lower an electric peak demand over a prediction horizon. In addition, note that δ is dependent on all sequences of stages of n-units. Therefore, it is clear that the control problem supervises all units. Γ_l and Γ_u are used for upper and lower bound comfort violations from the first constraint of (6).

Note also that we only want to regulate the N_p-step ahead predicted temperatures within a temperature bound and not each of the predicted temperatures for less than the N_p-steps. This is acceptable because our prediction horizon, N_p, is relatively short, e.g. 30 min to 1 hour. The N_p-step temperature regulation reduces the large number of inequality constraints that would be necessary if all of the predicted temperatures were constrained.

The original RTU Coordinator presented by Kim et al. (2015) utilized a somewhat different cost function that didn't include the peak demand limit (second term) and deviations from upper and lower temperature bounds (third and fourth terms) in (5). The addition of the second term in (5) along with the second constraint of (6) improves the performance of the algorithm in terms of peak demand reduction when applied to buildings that don't have spaces that are closely coupled (e.g., office spaces). The addition of the third and fourth terms in (5) along with their use in the first constraint of (6) provides additional freedom for trading off power consumption and comfort.

3.3.2. Control Challenge and Augmentation of a Disturbance Model

Unmeasured disturbances can deteriorate performance of a controller, if those are not treated appropriately. To handle the problem, we adopt a well-known method, the *internal model principle* (Francis and Wonham, 1976) which is applied in various control fields, e.g. adaptive controls (Åström and Wittenmark, 2013) and process controls (Maeder et al., 2009; Muske and Badgwell, 2002; Pannocchia and Rawlings, 2003). The idea is fundamentally the same as the treatment of unmeasured disturbance in modeling, saying "Include a disturbance model internally to handle (or reject) disturbances". More precisely, the method augments a system model with a disturbance model to compensate for the modeling error and disturbances. In our case, it has the following form.

$$\begin{bmatrix} T(k+1) \\ \zeta(k+1) \end{bmatrix} = \begin{bmatrix} A & B_d \\ 0 & I \end{bmatrix} \begin{bmatrix} T(k) \\ \zeta(k) \end{bmatrix} + \begin{bmatrix} B_u \\ 0 \end{bmatrix} u(k) + w(k) \tag{7}$$

$$y(k) = \begin{bmatrix} C & C_d \end{bmatrix} \begin{bmatrix} T(k) \\ \zeta(k) \end{bmatrix} + \nu(k), \tag{8}$$

where w and ν are white noise processes having covariance matrices of Q, R, respectively. A, B_u, C are estimated from the identification approach (see (4)). The integrating mode, ζ, which is not *controllable* but *observable*, represents the unknowns. In general, the parameters of (B_d, C_d) have to be adjusted depending on the system of interest.

With the assumption of slowly varying output disturbances, we chose a simple but widely used solution (Muske and Badgwell, 2002) that can be achieved by letting $B_d = 0$ and $C_d = I$. For a stable system, as in our building system,

the constant output disturbance model removes steady state offset caused by the model mismatch and the unmodeled disturbances (Qin and Badgwell, 2003).

For notation simplicity,

$$A_a := \begin{bmatrix} A & 0 \\ 0 & I \end{bmatrix}, B_a := \begin{bmatrix} B \\ 0 \end{bmatrix}, C_a := \begin{bmatrix} C & I \end{bmatrix}, x_a := \begin{bmatrix} T \\ \zeta \end{bmatrix}. \tag{9}$$

If (A, C) is *detectable*[3], then the augmented system (A_a, C_a) is detectable since the integrating mode ζ is always 'recorded' in y. Furthermore since (A, C) is *observable*, the augmented system is automatically detectable. With the assumption of *stabilizability* of $(A_a, \sqrt{Q})$, the *detectabilty* ensures that a steady Kalman filter exists and is stable (See Anderson and Moore (2012) for the proof). Then the Kalman gain, denoted as K_a, for the augmented system, can be obtained by solving the following algebraic *Ricatti* equation.

$$P = A_a^T(P - PC_a^T(R + C_aPC_a^T)^{-1}C_aP)A_a + Q \tag{10}$$

Therefore our final model for MPC is

$$\begin{aligned} \hat{x}_a(k+1) &= A_a\hat{x}_a(k) + B_au(k) + K_ae(k) \\ y(k) &= C_a\hat{x}_a(k) + e(k). \end{aligned} \tag{11}$$

where $K_a = A_aPC_a^T(R + C_aPC_a^T)^{-1}$ and $e(k) = y(k) - \hat{y}(k|k-1)$.

3.3.3. Control Algorithm

With the modified model (11) to handle disturbances, the optimization problem of (5) and (6) can be now formulated in an implementable form as follows.

$$\min_{U,\delta,\Gamma_l,\Gamma_u} \quad \vec{P}^TU + d\delta + c_l\Gamma_l + c_u\Gamma_u \tag{12}$$

$$\begin{bmatrix} \tilde{P} & -\vec{1} & & \\ \mathcal{M} & & -\vec{1} & \\ -\mathcal{M} & & & \vec{1} \end{bmatrix} \begin{bmatrix} U \\ \delta \\ \Gamma_l \\ \Gamma_u \end{bmatrix} = \begin{bmatrix} \vec{0} \\ T_u - \mathcal{O}\hat{x}_a(k|k-1) \\ -T_l + \mathcal{O}\hat{x}_a(k|k-1) \end{bmatrix} \tag{13}$$

$$U_l \le U \le U_u \tag{14}$$

$$0 \le \delta \le \sum_{i=1}^{n} p_i \tag{15}$$

$$0 \le \Gamma_l \tag{16}$$

$$0 \le \Gamma_u \tag{17}$$

where $\vec{p} = [p_1, \cdots, p_n]^T, \vec{P} = [\vec{p}^T, \cdots, \vec{p}^T]^T$, $\tilde{P} = I_{N_p} \otimes \vec{p}^T$, $U = [u(k)^T, u(k+1)^T, \cdots, u(k+N_p-1)^T]^T$, $\mathcal{O} = C_aA_a^{N_p}$ and $\mathcal{M} = [C_aA_a^{N_p-1}B_a, C_aA_a^{N_p-2}B_a \cdots, C_aB_a]$.

[3]We say the pair (A, B) is *stabilizable* if (A, B) has no *uncontrollable* and *unstable* hidden modes. Similarly, the pair (A, C) is said *detectable* if (A, C) has no *unobservable* and *unstable* hidden modes (Callier and Desoer, 1991).

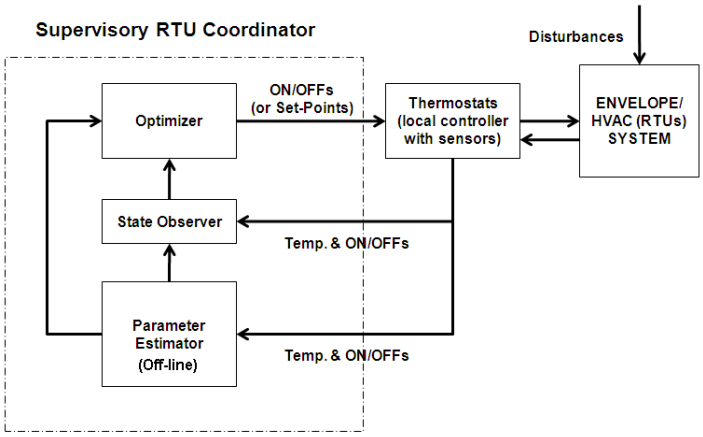

Figure 2: Basic structure of Unit Coordinator

$\hat{x}_a(k|k-1)$ is the estimated state at k through the Kalman filter for the augmented system in (11).

The optimal control problem has been converted to the standard linear programming form, and hence can be solved by a mixed integer linear programming solver (note that u is a vector of integers while the auxiliary variables are positive real numbers).

3.4. Summary of Supervisory Controller and Further Discussions

A basic control structure is shown in Fig. 2 which has a standard form of the model based controller. The parameter estimator was explained in Section 3.2 and (11) is the state observer in this figure. The observer provides an estimated state, i.e. $\hat{x}_a$, and allows the optimizer to solve the control objective from (12) to (17). The parameter estimator was implemented off-line on a prepared dataset (one or two weeks of data), while the other algorithms were implemented on-line to handle model uncertainties and real-time disturbances.

Handling unmeasured building heat gains is focused on designing a reliable MPC by rejecting disturbances in the modeling phase and by considering them in the control phase. We call the complete MPC solution the Unit Coordinator (UC).

T_o is included in the identification process to provide measured disturbance information but is excluded in the control phase due to narrow prediction horizon. The use of only thermostat outputs as input measurements for the coordination algorithm is an important feature that enables a scalable and low-cost implementation. However, due to the lack of other disturbance information, only a short prediction horizon, say less than an hour, is feasible. The short prediction horizon restricts an active usage of the building's thermal mass and it is a limitation of the controller.

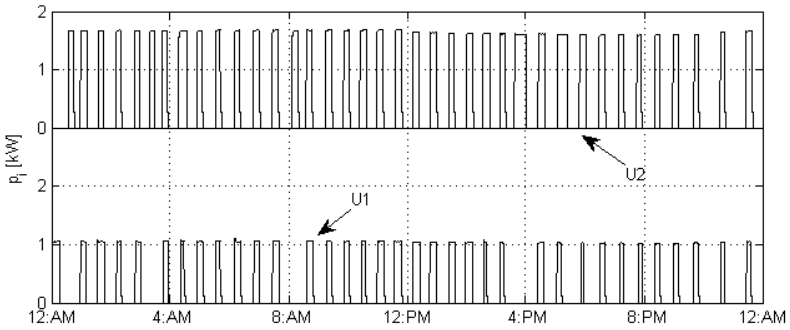

Figure 3: Examples of unit power profiles for 2 days (1 min sampling time)

4. Site Performance of a MPC for RTU coordination

The presented MPC has been implemented at existing buildings, and example results are shown in this section. In Section 4.2, test results for a laboratory environment are presented which clearly show benefits of the MPC compared with a conventional thermostat control. In Section 4.3, site performance of the MPC for a small retail store is presented.

4.1. Measurement Setup

Thermostat temperatures, humidities, unit run times (over a 5 min interval) were recorded using web-enabled thermostats with a 5 min sampling time for the laboratory set up and a small retail store. The thermostat employed for experiments provides the compressor run time(s) over a 5 min interval rather than the instantaneous stage(s). Therefore, the unit stage was estimated by dividing the thermostat run time data by 5 min resulting in a real number rather than an integer. The estimation error should be negligible for most times, since both RTUs and thermostats have anti-cycling clocks ($\approx 5min$) to prevent a significant short cycling that is harmful for compressors. The outdoor air temperature was obtained from a NOAA (National Oceanic and Atmospheric Administration) website.

It should be mentioned that it was not possible to install power measurements for the RTUs at the field site. Instead, rated powers from manufacturers' data and measured run time were used to estimate energy consumption for each RTU. To test the reliability of the simple power estimation approach, current transducers (CT) were installed to measure currents for two packaged units in the laboratory environment and measurements were compared with the simple estimation approach. They convert true RMS 10/20/50 amps, depending on the selection of a range jumper, to 0-5 VDC for a single phase AC power. The accuracy is ± 1 % of 10 amps. The data is recorded through an Arduino board for every 1 min. Unit powers were estimated using the CT with an assumption that the power factors and RMS voltage are reasonably constant.

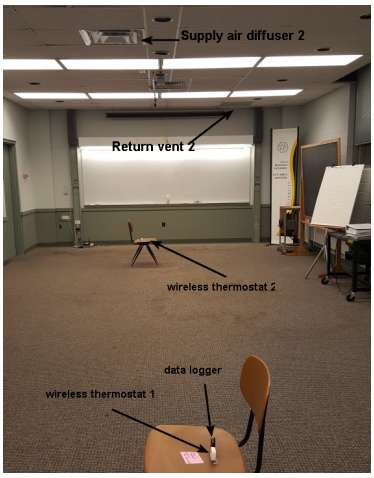

Figure 4: Case study building (supply air diffuser 1 and return vent 1 are not shown)

Fig. 3 displays the power behavior for each unit (denoted as U1 and U2) individually for example days. Once the compressor is ON, the unit power stabilizes quickly (< 1 min) to a relatively constant value that doesn't vary much over the course of the day with changing indoor and outdoor conditions. Thus, the power is primarily correlated with the compressor status. These results support the validity of the simple approach for estimating power consumption of fixed speed units.

4.2. Case 1: Laboratory Environment

4.2.1. Building Description

To test the overall MPC approach in terms of both the modeling and control algorithms, a cooling system for a conference room (about 15 m long, 7 m wide and 3.5 m high) in the Ray W. Herrick Laboratories at Purdue University, IN, U.S. (see Fig. 4) was retrofitted. Two packaged air conditioners (termed U1 and U2) having different cooling capacities were installed and the air duct system was reconfigured accordingly. U1 is a 1-ton single stage unit with an energy efficiency ratio (EER) 9 and U2 is a 2-ton single stage unit with 10 EER. Thermostats, supply and return vents associated with the two units are shown in Fig. 4 and Fig. 5. In this system, we have 2 thermostat temperature outputs and 3 measured inputs that are the unit stages and outdoor air temperature. Note that there is a strong coupling between the two sub-zones (or thermostats), and hence the operation of one unit can influence both thermostat temperatures. Unmeasured heat sources are lighting gains (around 1.5 kW), loads from electric appliances (a small freezer and one laptop computer), infiltration/exfiltration and solar gains though windows. The lights were turned ON and OFF by occupant random behavior.

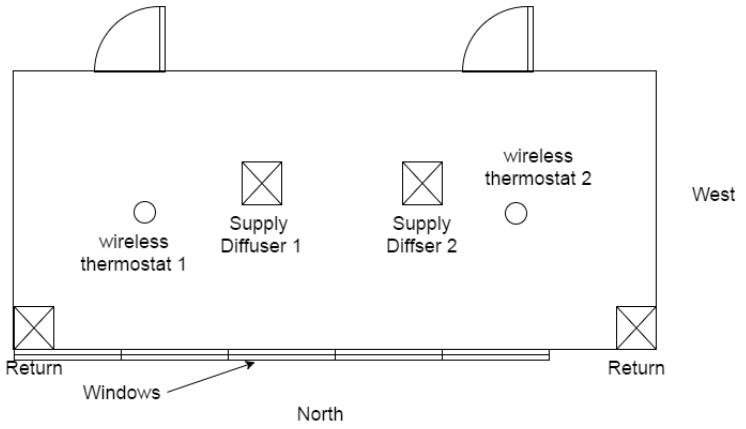

Figure 5: Floor plan with locations of thermostats, supply and return vents (Purdue Herrick Laboratory)

4.2.2. Experiment Setup

During the experiments, supply fans were cycled on and off with compressor stages (auto fan mode) for the two units. The sampling time for control implementation was 5 minutes and the prediction horizon was set to 1 hour. Thermostat setpoints were set to 22.2 ^oC (72 ^oF) for both thermostats for all times. The setpoints were used for the upper bound (T_u) in (6) with a temperature band of 2.22 ^oC (4 ^oF), i.e. $T_l = T_u - 2.22$ (^oC). For the penalty terms of δ and (Γ_l, Γ_u), 100 and 1000 values were assigned in this experiment. These weights were determined through iteration and were found to work well for all of the demonstration sites in terms of minimizing demand while maintaining thermostat temperatures near their setpoints. The MPC was implemented on the control platform shown in Fig. 1.

4.2.3. Test Results of MPC in a Laboratory Environment

Validation results associated with the modeling approach are presented in Kim et al. (2018), and hence we provide only a brief summary and a concluding result in this paper. The primary focus is on performance of the MPC.

The data sets for model training were generated by perturbing setpoints using a pseudo random binary signal (PRBS). The magnitude of the setpoint perturbation level was bounded to 2.22^oC (4^oF) for daytime and 4.44^oC (8^oF) for nighttime. The information of outdoor air temperature was obtained from NOAA (National Oceanic and Atmospheric Agency) weather data with a one hour sampling time. The hourly outdoor air temperature data was interpolated for the 5-minute sampling time. A grey-box model was developed using the proposed identification algorithm. To validate the result, several step tests were performed and are compared with the predicted step response using the model. Fig. 6 shows the comparison result. The two figures at the left hand side describe how the two thermostat temperatures of the two units (U1 and U2) drop when

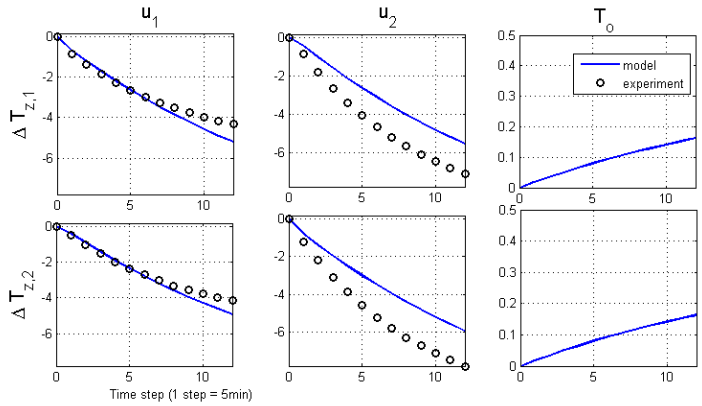

Figure 6: Model comparisons with experimental step test results (1 step = 5min)

U1 tunes on for an hour. The dotted lines represent experimental step tests (averaged) and the blue solid lines indicate the model responses. The middle figures show responses under U2, and the right figures indicate how temperatures increase when T_o increases for 1^oC.

The estimated model matches experiments reasonably well, despite the lack of heat gain measurements as inputs. For more comprehensive descriptions and results, and for comparisons to a conventional grey-box identification approach, refer to Kim et al. (2018).

The model was applied in the MPC algorithm after the augmentation discussed in Section 3.3.2. Fig. 7 shows sample responses of thermostat temperatures (second), relative humidities (third), unit staging (fourth) and total HVAC power (last) associated with conventional control and the MPC (Unit Coordinator, UC) for the laboratory testing. The testing involved switching between the Unit Coordinator (UC) and conventional control at irregular intervals as indicated in the bottom sub-figure. The unit stages were estimated by scaling the measured compressor run times over a 5 min sampling period. At the middle of Sep/16 in the second subfigure, there is a slight temperature jump associated with the UC (see the blue arrow). This is because of a small modification of a control parameter T_u at the time. Note that averaged zone temperatures of the UC before the time are up to 1 ^oC lower than those of the conventional control (Sep/15). This is because the conventional thermostat control regulates temperatures around the setpoints (22.2 ^oC) while the UC regulates temperatures below the 22.2 ^oC upper bound. This mean temperature bias could underestimate performance of the UC and so the parameter T_u was slightly adjusted ($< 1^oC$) to have similar mean temperatures.

Note that there are clear distinct behaviors of the two controllers in terms of the electric demand shown in the last sub-figure. Note also that both controllers maintain zone temperatures near the setpoints (22.2 ^oC) in the first sub-figure. The conventional thermostat control caused high electric demands for most

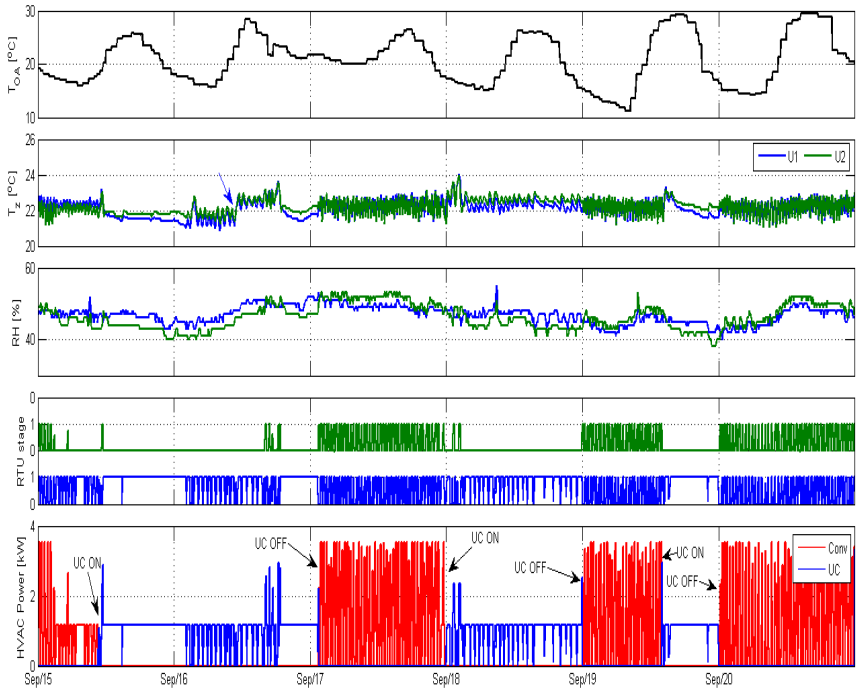

Figure 7: Profiles of thermostat temperatures and humidities, unit cyclings and total HVAC power for conventional and the MPC at a laboratory environment

times, due to simultaneous operation of the two units as shown in the third sub-figure. This high correlation of operation of the two units is caused by the significant inter-zonal coupling through the open area (See Fig. 5). On the other hand, the proposed MPC (UC) reduced electric demands significantly (over 50 % for most times) compared with the conventional case despite the strong coupling. It demonstrates that the MPC properly captures the dynamics of the building system.

From the experimental results, it is also clear that a conventional thermostat control algorithm causes an unnecessarily high demand even under significantly low part load conditions. This can be confirmed for the data on September 18 and 19. Note that the MPC utilized only U1 (1-ton unit) during the day time on Sept 18 (see the third sub-figure), while the conventional control used both units (totally 3-ton) for both day time and night time on Sept 19.

Fig. 7 shows the conventional control led to a significantly short unit cycling (see the last sub-figure) due to the strong inter-zonal interaction, while the UC led to less cycling due to a clear tendency to utilize U1[4]. Short cycling can lead to over cooling of a space due to minimum compressor run times and increased total energy consumption due to decreased efficiency associated with more on/off cycling (cyclic degradation phenomena (Henderson et al., 2000; Katipamula and O'Neal, 1992)). The relative energy savings of the UC for the test period is about 14 %. Therefore, the performance of the MPC is superior to that of the conventional control in terms of energy consumption, life of the compressors, and electric peak demand.

Although relative humidity is not a controlled variable and the MPC does not account for it, it is important to mention that the MPC had similar relative humidities (at the thermostats) with the conventional control.

4.3. Case 2: Performance of MPC at a Site

4.3.1. Strategy to Evaluate Performance of MPC

A fair comparison of performance between two controllers over a long period of time on an existing building is challenging, because the controller performance highly depends on the building loads that can vary significantly from day to day. Recall that internal gains, which are stochastic, account for a significant portion of the total building load for commercial buildings. Our strategy to fairly compare performance between the proposed MPC and a conventional thermostat control is to switch back and forth between the two controllers on a daily basis. That is, one controller was enabled on even days while the other controller was run on odd days. The switching process was repeated at the test sites for a long time period and, for each day, daily RTU energy usage and electric peak demand were obtained.

[4]The preference of the UC may be explained from the estimated model and rated powers specified in the MPC objective function. Note that the UC thinks the two temperatures can be dropped to similar magnitudes using U1 (compare step responses of U1 and U2 for the model in Fig 6) but with smaller energy.

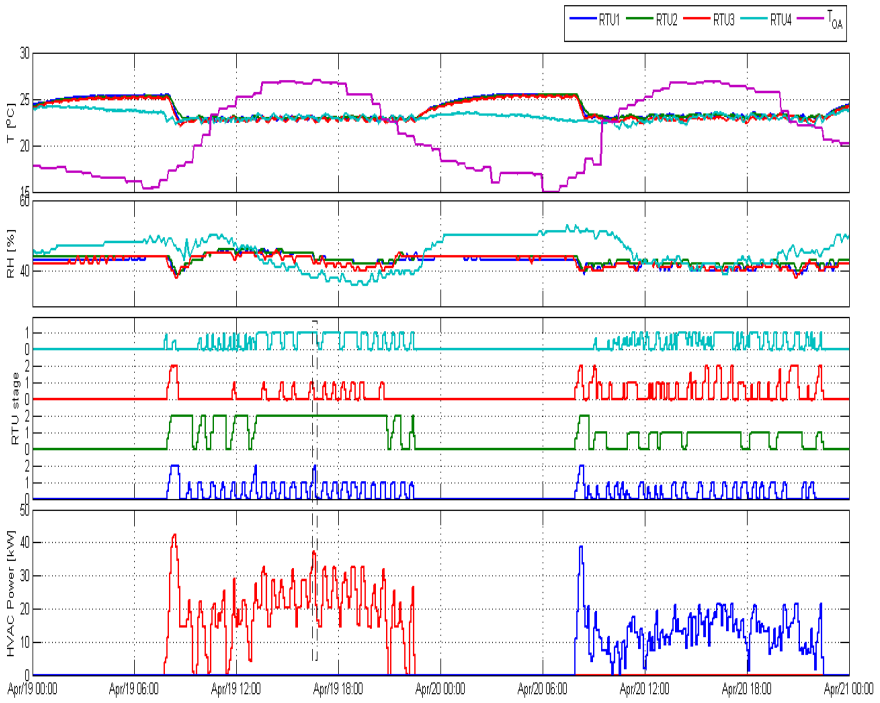

Figure 8: Profiles of thermostat temperatures and humidities, RTU cyclings and total HVAC power for the conventional and MPC at a field site

4.3.2. Building Description and Experimental Setup

A small retail store (floor area around 1,400 m^2, $15,000 ft^2$) is a demonstration site located in Florida. The building has 4 RTUs where three of them, named RTU1-3, serve a main open service area and one RTU, named RTU4, serves a storage room. RTU1, RTU2 and RTU3 are 18, 15 and 8-ton two-stage units respectively, and RTU4 is a 5-ton single-stage unit. Each of the RTUs has its own thermostat that controls a local zone. For this project, the original thermostats were replaced with web-enabled thermostats that have an open API. The experimental setup is described in Section 4.1. The MPC and conventional controller were implemented using the control architecture of Fig. 1 with the MPC server located in Pennsylvania.

The same configurations for controllers described in Section 4.2.2 were used for this demonstration, except that thermostat setpoints were adjusted by fixed schedules for night setup: 22.8 ^oC (73 ^oF) for an occupied period and 26.6 ^oC (80 ^oF) for an unoccupied period. Users were allowed to turn the schedule mode on or off or to override the scheduled setpoints.

4.3.3. Short-term Evaluation Results

A sample comparison for the small retail store building from experiments is shown in Fig. 8. The control strategy was toggled from the conventional thermostat control (Apr/19, Tuesday) to the MPC unit coordinator (Apr/20, Wednesday). Fig. 8 shows responses of thermostat temperatures and humidities, RTU staging and total estimated HVAC power for the site associated with conventional control and the MPC coordinator for the two different days having similar ambient conditions (marked as purple line).

It can be seen that the highest electric demand occurred from 8 to 9 AM for both controllers. This is because of the night setup schedule which abruptly changes setpoints for all thermostats as shown in the temperature plot. This peak was removed by adding a low pass filter, e.g. a moving average filter, to the setpoint schedule signals for both controllers and the corresponding results are shown in the following section.

Consider the conventional control results at around 4 PM, marked with a dashed box, where RTUs 1, 2, and 4 were all operating at their maximum stages. As a result of this, a high electric peak demand occurred at this time. On the other hand, there is a clear tendency that the MPC coordinates the RTUs so that not all units operate at the same time. It can be checked by comparing stages of RTU1 and RTU3 (RTU1 and RTU3 were operating at different times). This results in electric peak demand reduction of about 50% (from around 40kW to around 20 kW) if we do not count the HVAC power peaks for the returning period of night setup. It is important to mention that temperatures were regulated at around the setpoint and relative humidities were also in a reasonable range for both controllers.

The total HVAC energy consumption for the day with the UC operation is significantly lower for the example results in Fig. 8. However, since this is only a short-term comparison, there could be significant differences in heat gains (e.g. plug and lighting loads, occupancy, and transmitted solar radiation). More definitive energy savings results for longer term tests are presented in Section 4.3.4.

4.3.4. Long-term Evaluation Results

Experimental results over a month (June) are shown in Fig. 9. First of all, the first sub-figure shows both controllers regulated temperatures in a reasonable range for the experimental period. Table 1 summarizes the mean and standard deviation of each thermostat temperature during the occupied period for the June test. There were no discernible differences in zone temperatures between the days under the Unit Coordinator (UC) and conventional control. This demonstrates robustness of the proposed algorithm with respect to unknown disturbances and changes of setpoints (remember that the demonstration site is a retail shop and thus has a highly stochastic internal gain profile, and user(s) could randomly change setpoints). Although the temperature of RTU4 that serves a storage (marked with sky color) is away from the setpoint (22.7 ^oC, 73 ^oF during an occupied period), it is because RTU4 was undersized

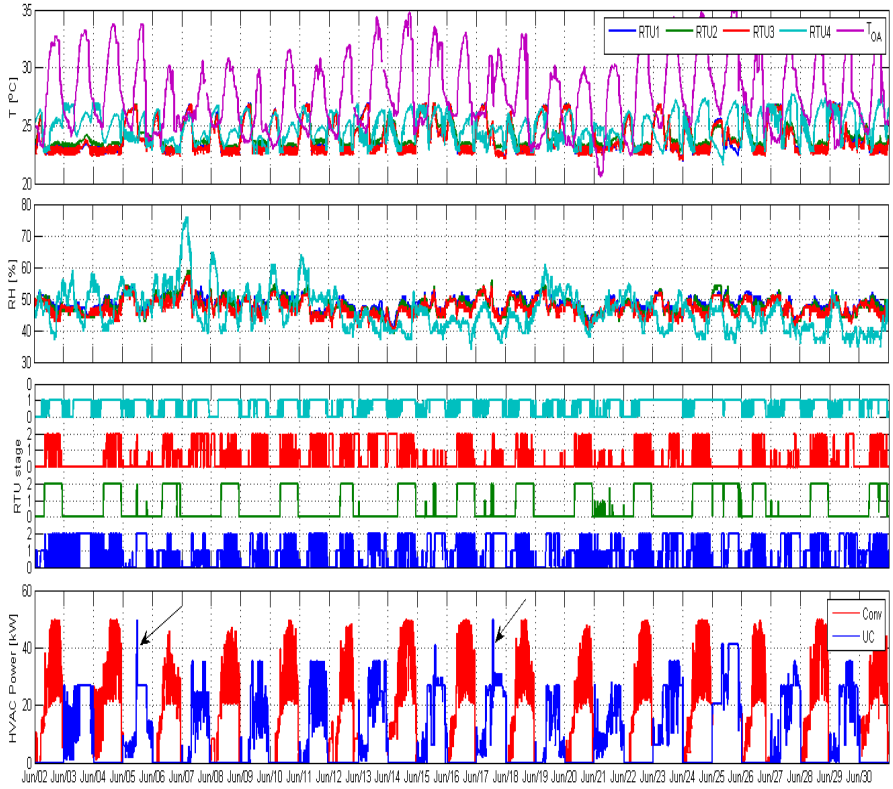

Figure 9: Profiles of thermostat temperatures, RTU cyclings and total HVAC power for the conventional and MPC at a field site

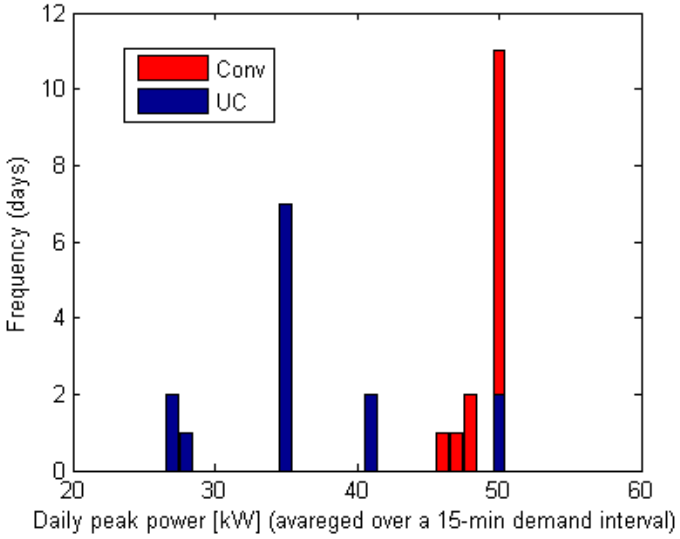

Figure 10: Histograms of daily peak demand for the June test period for a small retail store

Controller	metric	RTU1	RTU2	RTU3	RTU4
Conv	mean	23.0	23.4	23.0	25.4
UC	mean	23.4	23.9	23.4	25.4
Conv	std	0.2	0.2	0.3	1.1
UC	std	0.5	0.5	0.6	1.2

Table 1: Mean and standard deviation [^oC] of thermostat temperatures during occupied period for the June test

(see the operating stage of RTU4) and hence the temperature violations were unavoidable for both controllers.

From the last figure, as expected, the conventional control led to much higher electric demands compared with the UC. For a clearer image of how the MPC differs from the conventional control, histograms of the peak power over a day for both controllers are shown in Fig. 10. For the calculation of the daily peak power, a 15-min moving average was applied to the HVAC power under the assumption of the 15-min demand interval, and then the maximum value for each day was calculated. The daily peak powers for the conventional and MPC controls distribute around 50 kW and 35 kW, respectively.

There are two points where the MPC caused peak demands of about 50 kW (see arrowed points in Fig. 9). However, this was caused by users' abrupt temperature setpoint changes that can be confirmed from the temperature profiles at those points. In general, the conventional thermostat control leads to unnecessarily high electric demand compared to the MPC even under part-load conditions. At part-load, the high electrical demand for conventional control is

Controller	RTU1	RTU2	RTU3	RTU4
Conv	68.1	4.1	48.8	40.7
UC	40.3	5.8	23.1	45.1

Table 2: Number of compressor stage changes (daily avergaed) for the June test period for a small retail store

	Apr	May	June	July
Energy Savings	12.6	13.8	12.8	12.6
Demand Savings	3.7	18.2	16.8	19.1

Table 3: Summary of relative savings [%] over a 4-month test period for a small retail store

a result of compressor short cycling. The number of unit stage changes (daily averaged) for each unit, i.e. how frequently unit stage is switched for a day, is shown in Table 2. Since the compressor run time over a 5 min is available rather than the compressor ON/OFF status, the run time was rounded to count the number of cycles. Overall, significant reductions of mode changes through the MPC are confirmed from the table. As discussed in the laboratory test section, energy savings for the UC with reduced short cycling and runtimes is expected.

Although relative humidity is not a controlled variable and the MPC does not account for it, it is important to mention that the MPC has similar relative humidities as the conventional control (at the thermostat locations).

Table 3 summaries the monthly savings of electrical energy and peak demand over a 4-month (Apr-July) test period. The strategy switched between the UC and conventional control each day over this entire period. The electric demand savings for each month was determined by comparing the peak HVAC power consumption determined from a 15-minute moving-average[5] for days under UC control with the peak for conventional control. Recall that it is possible to have unnecessarily high peak demands because of users' abrupt setpoint changes. Outliers for this site occurred on a few days for each month but tend to bias the savings in a random manner if they are included in the monthly peak demand calculation. Therefore, we neglected outliers due to user setpoint changes in calculating demand savings for each month. The issue of users' abrupt setpoint change was resolved by using the same moving average approach discussed in section 4.3.3, but the results presented in this paper did not include this improvement.

The MPC provided consistent energy savings at around 12% and demand savings around 18%. During the April, the demand savings were much lower than the other months. This is because of the night-setup issue discussed in

[5]It is typical in U.S. that the demand bill is calculated from averaged power over a demand interval (5, 10 and 15 min are common) rather than an instantaneous power. Therefore, the demand savings calculated from the 15-moving average could underestimate those with shorter demand intervals.

Section 4.3.3. Once a moving average was added to the night-setup schedule, the issue was resolved and consistent demand savings were achieved.

5. Discussion and Conclusions

Despite the large number of SMCBs in this country, few advanced control algorithms have been developed for packaged air conditioners that are typically used in these applications. The challenge is that low cost control solutions are needed that don't have significant configuration requirements. This paper presented and demonstrated a complete MPC solution for coordinating multiple packaged air conditioners at a given site that has the potential for implementation at low cost. It includes an identification algorithm, control algorithm, and control infrastructure. Experimental results were presented for both a laboratory environment and field site. The controller only requires inputs from the thermostats and handles unknown disturbances caused by lack of sensor points using a lumped disturbance model. The reliability of the controller has been demonstrated through implementation and testing at a field site for 4 months. The controller consistently showed about 12% HVAC energy savings and about 18% HVAC peak demand reduction compared with a conventional thermostat algorithm.

A cloud-based implementation for the RTU controller, such as the one presented in this paper, would seem to be at logical commercialization approach for retrofit in many SMBCS because of the widespread availability of web-enabled thermostats. This type of solution is particularly attractive for individual small commercial buildings that don't have a building automation system (BAS), which is much of the small commercial buildings world. If the process of learning models were automated, then the primary costs for implementation of the coordinator would be retrofitting thermostats with web-enabled versions and connecting them to the cloud through existing WiFi. An alternative approach could involve integration of the RTU coordination software within hardware that is connected between thermostats and the RTUs at the site. This would eliminate the need for an internet connection and would be widely applicable to small commercial buildings that don't have a BAS. The algorithms could also be embedded at the factory within smart RTU controllers as long as individual RTU controllers could talk to each other at a site. For enterprise solutions (e.g., national chains), the solution could be implemented on top of or within existing BASs. The overall economics could be quite favorable for large national chains with standardized BAS solutions because once implemented the RTU coordinator could be delivered at a large scale across many installations. This is an attractive initial application for this control algorithm. In the longer term, the RTU coordinator could be implemented as a standard application within BASs.

6. ACKNOWLEDGMENTS

The authors wish to thank Dr. Todd Rossi, Pallav Negi, Jason Blum, Timothy Stockman and Allen Cross from mCloud Inc. for their valuable suggestions

and support for field site demonstrations of the MPC. The work was supported by Center for High Performance Building (CHPB) at Purdue University.

7. NOMENCLATURE

SMCB: small and medium-sized commercial buildings

UC : unit coordinator

BAS: building automation system

RTU: rooftop unit

IO: inputs and outputs

NOAA: national oceanic and atmospheric administration

CT: current transducer

RMS: root mean squares

EER: energy efficiency ratio

HVAC: heating, ventilating, and air conditioning

n **:** number of RTUs

y **:** vector of thermostat temperatures

u **:** vector of RTU compressor stages

T_o **:** outdoor air temperature

m **:** number of measured inputs

G_u **:** dynamic system that maps u to y

G_{T_o} **:** dynamic system that maps T_o to y

$\dot{Q}_g$ **:** unmeasured heat gains

v **:** lumped output disturbances

H **:** dynamics of lumped output disturbances

e **:** white noise

θ **:** physical parameters consisting of thermal resistances and capacitances

ρ **:** parameters that constructs dynamics of lumped output disturbances, i.e. H

$\big(A(\cdot), B_u(\cdot), B_{T_o}(\cdot), C(\cdot)\big)$ **:** a state space model structure that maps θ to building dynamics, i.e. G_u and G_{T_o}

$(\mathcal{F}(\cdot), \mathcal{G}(\cdot))$ **:** a state space model structure that maps ρ to lumped disturbance dynamics , i.e. H

(A_a, B_a, C_a) **:** aggregated dynamic system matrices

K_a **:** Kalman gain

k **:** current time step

j **:** prediction time step

N_p **:** prediction horizon

δ **:** an upper bound of instantaneous power

(Γ_l, Γ_u) **:** temperature violations from lower and upper temperature bounds

(T_l, T_u)**:** lower and upper temperature bounds

(c_l, c_u)**:** weights on optimization variables for (Γ_l, Γ_u)

d **:** weight on optimization variables for δ

ζ**:** internal state of lumped output disturbances

$\hat{x}_a$**:** aggregated state that includes building temperatures and internal state of disturbances

e**:** one step ahead prediction error

u_i**:** i^{th} unit stage

p_i**:** i^{th} unit power

$\vec{1}$**:** a column vector whose components are the unity.

8. REFERENCES

References

Andersen, K.K., Madsen, H., Hansen, L.H., 2000. Modelling the heat dynamics of a building using stochastic differential equations. Energy and Buildings 31, 13–24.

Anderson, B.D., Moore, J.B., 2012. Optimal filtering. Courier Dover Publications.

Åström, K.J., Wittenmark, B., 2013. Adaptive control. Courier Dover Publications.

Biyik, E., Brooks, J.D., Sehgal, H., Shah, J., Gency, S., 2015. Cloud-based model predictive building thermostatic controls of commercial buildings: Algorithm and implementation, in: American Control Conference (ACC), 2015, IEEE. pp. 1683–1688.

Braun, J.E., Montgomery, K.W., Chaturvedi, N., 2001. Evaluating the performance of building thermal mass control strategies. HVAC&R Research 7, 403–428.

Callier, F.M., Desoer, C., 1991. Linear system theory (springer texts in electrical engineering) .

Chen, X., Wang, Q., Srebric, J., 2015. Model predictive control for indoor thermal comfort and energy optimization using occupant feedback. Energy and Buildings 102, 357–369.

DOE, U., 2009. Buildings energy data book. US Department of Energy. URL: http://buildingsdatabook.eere.energy.gov/.

Dong, B., Lam, K.P., Neuman, C., 2011. Integrated building control based on occupant behavior pattern detection and local weather forecasting, in: Twelfth International IBPSA Conference. Sydney: IBPSA Australia, pp. 14–17.

Forssell, U., Ljung, L., 1999. Closed-loop identification revisited. Automatica 35, 1215–1241. URL: http://www.sciencedirect.com/science/article/pii/S0005109899000229.

Fraisse, G., Viardot, C., Lafabrie, O., Achard, G., 2002. Development of a simplified and accurate building model based on electrical analogy. Energy and buildings 34, 1017–1031.

Francis, B.A., Wonham, W.M., 1976. The internal model principle of control theory. Automatica 12, 457–465.

Harb, H., Boyanov, N., Hernandez, L., Streblow, R., Müller, D., 2016. Development and validation of grey-box models for forecasting the thermal response of occupied buildings. Energy and Buildings 117, 199–207.

Henderson, H.I., Parker, D., Huang, Y.J., 2000. Improving doe-2's resys routine: User defined functions to provide more accurate part load energy use and humidity predictions. Lawrence Berkeley National Laboratory .

Van den Hof, P., 1998. Closed-loop issues in system identification. Annual reviews in control 22, 173–186. URL: http://www.sciencedirect.com/science/article/pii/S1367578898000169.

Katipamula, S., O'Neal, D.L., 1992. A part load factor for a heat pump derived from laboratory measurements. Energy and buildings 19, 125–132.

Katipamula, S., Underhill, R.M., Goddard, J.K., Taasevigen, D., Piette, M., Granderson, J., Brown, R.E., Lanzisera, S.M., Kuruganti, T., 2012. Small- and medium-sized commercial building monitoring and controls needs: A scoping study. Pacific Northwest National Laboratory (PNNL), Richland, WA (US), Tech. Rep .

Kim, D., Braun, J., Cai, J., Fugate, D., 2015. Development and experimental demonstration of a plug-and-play multiple rtu coordination control algorithm for small/medium commercial buildings. Energy and Buildings 107, 279–293.

Kim, D., Cai, J., Ariyur, K.B., Braun, J.E., 2016. System identification for building thermal systems under the presence of unmeasured disturbances in closed loop operation: Lumped disturbance modeling approach. Building and Environment 107, 169–180.

Kim, D., Cai, J., Braun, J.E., Ariyur, K.B., 2018. System identification for building thermal systems under the presence of unmeasured disturbances in closed loop operation: Theoretical analysis and application. Energy and Buildings 167, 359 – 369. URL: http://www.sciencedirect.com/science/article/pii/S0378778817317322, doi:https://doi.org/10.1016/j.enbuild.2017.12.007.

Ljung, L. (Ed.), 1999. System Identification (2Nd Ed.): Theory for the User. Prentice Hall PTR, Upper Saddle River, NJ, USA.

Ljung, L., McKelvey, T., 1996. Subspace identification from closed loop data. Signal Processing 52, 209–215. URL: http://www.sciencedirect.com/science/article/pii/0165168496000540.

Maeder, U., Borrelli, F., Morari, M., 2009. Linear offset-free model predictive control. Automatica 45, 2214–2222. URL: http://www.sciencedirect.com/science/article/pii/S0005109809002969.

Muske, K.R., Badgwell, T.A., 2002. Disturbance modeling for offset-free linear model predictive control. Journal of Process Control 12, 617–632. URL: http://www.sciencedirect.com/science/article/pii/S0959152401000518.

Pannocchia, G., Rawlings, J.B., 2003. Disturbance models for offset-free model-predictive control. AIChE Journal 49, 426–437. URL: http://onlinelibrary.wiley.com/doi/10.1002/aic.690490213/abstract.

Putta, V., Kim, D., Cai, J., Hu, J., Braun, J.E., 2015. A switched dynamic programming approach towards optimal control of multiple rooftop units, in: American Control Conference (ACC), 2015, IEEE. pp. 281–287.

Qin, S.J., Badgwell, T.A., 2003. A survey of industrial model predictive control technology. Control engineering practice 11, 733–764. URL: http://www.sciencedirect.com/science/article/pii/S0967066102001867.

Reynders, G., Diriken, J., Saelens, D., 2014. Quality of grey-box models and identified parameters as function of the accuracy of input and observation signals. Energy and Buildings 82, 263–274.

Rogers, D., Foster, M., Bingham, C., 2014. Experimental investigation of a recursive modelling mpc system for space heating within an occupied domestic dwelling. Building and Environment 72, 356–367.

Širokỳ, J., Oldewurtel, F., Cigler, J., Prívara, S., 2011. Experimental analysis of model predictive control for an energy efficient building heating system. Applied Energy 88, 3079–3087.

Söderström, T., Stoica, P., 1988. System identification. Prentice-Hall, Inc.

Van Overschee, P., De Moor, B., 1997. Closed loop subspace system identification, in: Decision and Control, 1997., Proceedings of the 36th IEEE Conference on, IEEE. pp. 1848–1853. URL: http://ieeexplore.ieee.org/xpls/abs_all.jsp?arnumber=657851.

Zhang, X., Pipattanasomporn, M., Rahman, S., 2017. A self-learning algorithm for coordinated control of rooftop units in small-and medium-sized commercial buildings. Applied Energy 205, 1034–1049.